



# FAST IN-CYLINDER PRESSURE RECONSTRUCTION FROM STRUCTURE-BORNE SOUND USING THE EM ALGORITHM

Ruben Villarino and Johann F. Böhme

Department of Electrical Engineering and Information Sciences  
Ruhr-Universität Bochum, D-44780 Bochum, Germany

## ABSTRACT

The paper addresses the problem of reconstructing the low-frequency part of in-cylinder pressure of spark ignition engines by analyzing structure-borne sound signals measured on the surface of the engine block. The new pressure trace model proposed yields accurate approximations with a minimal number of parameters. When combined with the EM algorithm, a processing scheme results that provides fast pressure estimates and efficiently exploits the information contained in the sound signal. Experimental results with real measurement data show the potential of the reconstructed signal to perform misfire detection and closed-loop spark ignition timing tasks.

## 1. INTRODUCTION

In-cylinder pressure has been used for many decades as a standard tool to examine the state of reciprocating internal combustion engines. The literature already contains numerous proposals that exploit the information-rich pressure trace for very different real-time diagnosis and control purposes, see e.g. [1]. However, despite its unquestioned potential, the high cost and limited lifetime of suitable sensors have relegated its use almost exclusively to the test bed, where it serves for both engine calibration as well as a performance reference for other methods.

In this respect, ion sensing has recently gained attention as a possible alternative. It consists of applying a DC bias to the spark plug when it is not used for ignition, and then measuring the current that flows through the circuit. Although it provides a direct insight into the processes playing in the combustion chamber, the ionization current is usually difficult to interpret, which limits its commercial application to misfire detection even though schemes for closed loop ignition timing already exist [2].

Structure-borne sound, obtained by accelerometers mounted on the surface of the engine block, can also be used to gather information about the engine's state. Apart from its reduced cost, the sound signal has the advantage of being able to monitor several cylinders simultaneously. Generally this is only possible at the expense of demanding signal processing procedures that suppress the interferences caused by the remaining engine aggregates. Nevertheless, structure-borne sound has already proven its usefulness in certain specific applications like knock detection, where in fact it has already established itself as the commercial standard in production engines.

In this context, the paper focuses on the reconstruction of the low-frequency part of the pressure trace by processing acceler-

---

This work was partially supported by Robert Bosch GmbH, Stuttgart, Germany.

meter signals, showing its potential to perform closed loop ignition control and misfire detection tasks. Wagner et al. [3, 4] have already carried out interesting work in this field. The procedure proposed in own paper also requires the prior identification of the transfer function between pressure and sound signal. However, this is not the main topic of the document and will be therefore briefly outlined after presenting a simplified signal model. The key contribution lies in the reconstruction procedure itself, which is based in another understanding of the combustion process and in using a new parametric model for the pressure traces. As it will be shown, the EM algorithm [5] fits into this framework, yielding fast estimates as well as providing additional flexibility for future improvements. Finally, the performance of the proposed method with real measurement data will be shown.

## 2. SOUND SIGNAL MODEL

Basically, the chosen approach relies on the assumption that the sound signal consists of a superposition of  $K$  different sound components, one for each cylinder, which are filtered versions of the corresponding pressure signals. By introducing  $q^{-1}$  as the left shift operator, i.e.  $q^{-m}y_n = y_{n-m}$ , the signal model can be written as

$$A(q^{-1})y_n = \sum_{k=1}^K H_k(q^{-1}, n)x_{k,n} + w_n, \quad (1)$$

or equivalently

$$y_n = (1 - A(q^{-1}))y_n + \sum_{k=1}^K H_k(q^{-1}, n)x_{k,n} + w_n. \quad (2)$$

This representation describes the measured sound signal  $y_n$  as the combination of three terms: a filtered version of past sound samples, with  $A(q^{-1}) = 1 + \sum_{m=1}^{M_A} a_m q^{-m}$ , a cylinder-dependant time-variant filtering  $H_k(q^{-1}, n)$  applied to each pressure component  $x_{k,n}$ , and a noise term  $w_n$  modelled as a white gaussian stochastic process of unknown variance  $\sigma_w^2$ .

Strictly speaking, the operator  $A(q^{-1})$  differs from the one employed in [4] since it is not based on any physical consideration. However, its inclusion into the model both simplifies the identification procedure and increases its performance, as experimental evidence shows.

The periodic movement of the piston motivates the use of time-variant transfer functions  $H_k(q^{-1}, n)$ . Assuming that the time-variant character of the system is described by the piston position  $z_{k,n} \in [z_{min}, z_{max}]$ , a first-order Taylor expansion around  $z_0$  yields

$$H_k(q^{-1}, n) \approx H_k^{(0)}(q^{-1}) + z_{k,n} \cdot H_k^{(1)}(q^{-1}), \quad (3)$$

where for simplicity and without loss of generality  $z_0 = 0$  was chosen. Accordingly,  $H_k(\cdot)$  combines two traditional LTI impulse responses, one of which is modulated by the piston position. Again, experimental evidence validates this approach: although higher orders could be included in (3), the proposed form represents a good trade-off between accuracy and computational load that adequately captures the behavior of the physical system, leading to parameter sets that are applicable over a wide range of engine speeds [4].

### 3. IDENTIFICATION

The identification of all  $K$  transfer functions must be carried out before addressing the reconstruction problem. Compared to [4], the structure of the signal model employed here facilitates the application of the prediction error method [6]. Since it is a standard procedure, it will be discussed briefly.

First, a one-step predictor for  $y_n$  is determined by taking the conditional expectation of (2) given all the past sound samples  $\mathcal{Y}^{n-1}$  and the pressure traces up to instant  $n$ ,  $\mathcal{U}^n$ . Since  $E\{w_n | \mathcal{Y}^{n-1}, \mathcal{U}^n\} = 0$ , it remains

$$\hat{y}_n = (1 - A(q^{-1}))y_n + \sum_{k=1}^K H_k(q^{-1}, n)x_{k,n}. \quad (4)$$

Second, the optimal filter coefficients  $\hat{A}(\cdot)$  and  $\hat{H}_k(\cdot)$  are obtained by minimizing the power of the prediction error  $\epsilon_n = y_n - \hat{y}_n$ ,

$$[\hat{A}, \hat{H}_1, \dots, \hat{H}_K] = \arg \min_{A, H_1, \dots, H_K} \frac{1}{N} \sum_{n=1}^N \epsilon_n^2. \quad (5)$$

When using FIR filters of length  $M_H$  for  $H_k^{(0)}(\cdot)$  and  $H_k^{(1)}(\cdot)$  in (3), equation (5) turns into a standard least-squares problem that can be solved straightforwardly. It yields fast estimates of the filter coefficients and also facilitates the combination of different data sets when speed and/or load-independent identification is required. However, these issues lie beyond the scope of this paper.

### 4. RECONSTRUCTION

Former sections have been aimed to introduce the reader to the somewhat peculiar sound model and to argue for the viability of the associated system identification. The rest of the document will consider that an adequate filter coefficient set is readily available.

The reconstruction of the pressure traces poses the problem of recovering multiple signals from a single sound source. In this SIMO framework, a direct inversion of the system is not possible and must therefore be circumvented.

Already [4] suggested to estimate the pressure by solving a fitting problem in the sound domain. This however supposes the availability of an adequate parametrization of the pressure curves and to know the exact information contained in each sound sample. Both issues are now addressed in detail.

#### 4.1. Pressure signal model

Some common properties arise among the pressure curves from different combustions when plotted against the crank angle  $\gamma$ . The signals always contain a component resulting from the compression of the air-fuel mixture that may vary in amplitude but usually shows the same shape. Concerning the pressure rise due to the

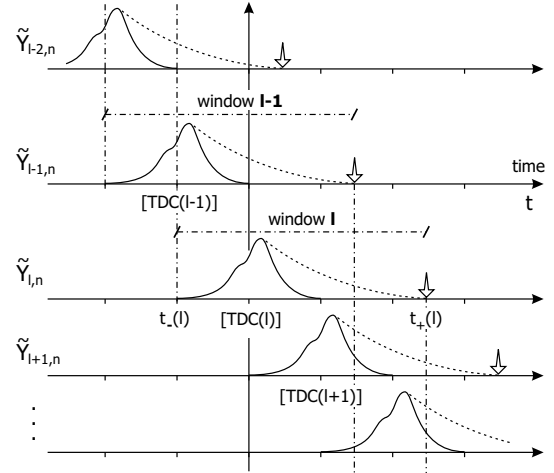


Fig. 1. Decomposition of the sound signal.

combustion itself it is observed that, while the maximum can always be found in a certain angular range after TDC (top dead center, the top upper piston position), the decay in the last part of the expansion stroke remains qualitatively the same. Some turbulence also shows up during the expulsion of the exhaust gases, but its effect will be neglected in a first approach.

The considerations above suggest to decompose the pressure trace in three parts: two pre-defined shapes, one associated with the compression and another one modelling the final phase of the combustion, and a third curve associated with the moving lobe. The proposed parametric model for a single combustion is then

$$x(\vartheta; \gamma) = \alpha_1 \cdot u_1(\gamma) + \alpha_2 \cdot u_2(\gamma) + \alpha_3 \cdot v(\gamma - \delta), \quad (6)$$

where  $\vartheta = (\alpha_1, \alpha_2, \alpha_3, \delta)'$  and  $x(\vartheta; \gamma) = 0$  outside the interval  $\gamma \in [-180^\circ, 180^\circ]$  around TDC. Section 5 will confirm that this approach actually yields satisfactory results.

#### 4.2. Sound signal decomposition

Since the goal is to estimate the pressure traces individually, it is more convenient to describe the sound as a summation over all combustions instead of over  $K$  cylinder-related signals as in (1). Accepting a slight abuse of notation in order to keep the expressions simple, the model reads now

$$\tilde{y}_n = A(q^{-1})y_n = \sum_{l=-\infty}^{\infty} \tilde{y}_{l,n}(\vartheta_l) + w_n \quad (7)$$

$$\tilde{y}_{l,n}(\vartheta_l) = H_l(q^{-1}, n)x_{l,n}(\vartheta_l) \quad (8)$$

where  $\tilde{y}_{l,n}(\vartheta_l)$  describes the effect of the single combustion  $x_{l,n}(\vartheta_l)$  in the sound domain, and the subindex of the transfer function is shorthand for ' $(l \bmod K) + 1$ '.

Although (8) holds true, in practice only a few combustions are actively involved in the sound perceived at a certain time instant. This is illustrated in figure 1 by plotting five different contributions of a 4-stroke engine one on top of another against the continuous time  $t$ . For each sound component, the pressure trace and the expansion caused by the filtering effect of the engine block are displayed, respectively, with a continuous and a dashed line. To simplify the drawing a constant motor speed was also assumed.

Consider now the task of estimating the pressure parameters  $\vartheta_l$  for the  $l$ -th signal. Intuitively, a data window between the starting

$t_-(l)$  and ending point  $t_+(l)$  of the combustion comprises all the relevant information for this task.

In order to find a suitable expression for these variables, let  $\gamma(t)$  describe the cumulative crank angle. It is a strictly monotonic increasing function of  $t$ , therefore its inverse  $\gamma^{-1}(\cdot)$  exists and can be used to connect both domains.

In a 4-stroke engine the combustions follow one another at  $720/K^\circ$  intervals. Let  $\gamma(0)$  be chosen, so that the crank angle for the piston at TDC on the compression stroke is given by  $\text{TDC}(l) = \frac{720}{K} \cdot l$ . Then, the limits for the  $l$ -th data window fulfill

$$t_-(l) = \gamma^{-1}(\text{TDC}(l) - 180) \quad (9)$$

$$t_+(l) = \gamma^{-1}(\text{TDC}(l) + 180) + T, \quad (10)$$

where  $T$  symbolizes the length of the transfer functions (3). Besides, the indices of the combustions covered by the data window will range from  $L_-(l)$  to  $L_+(l)$ , where

$$L_-(l) = \inf_{\lambda} \{t_-(l) < t_+(\lambda)\} \quad (11)$$

$$L_+(l) = \sup_{\lambda} \{t_-(\lambda) < t_+(l)\}. \quad (12)$$

Finally, defining  $n_-(l)$  and  $n_+(l)$  as the sample indices corresponding respectively to  $t_-(l)$  and  $t_+(l)$  in the discrete time domain for a given sample frequency  $f_s$ ,

$$n_-(l) = \lceil t_-(l) \cdot f_s \rceil, \quad n_+(l) = \lfloor t_+(l) \cdot f_s \rfloor, \quad (13)$$

an estimate for the vector parameter  $\underline{\vartheta}_l$  can be found by solving the following least-squares problem:

$$\min_{\underline{\vartheta}_{L_-(l)}, \dots, \underline{\vartheta}_{L_+(l)}} \sum_{n=n_-(l)}^{n=n_+(l)} \left| \tilde{y}_n - \sum_{m=L_-(l)}^{m=L_+(l)} \tilde{y}_{m,n}(\underline{\vartheta}_m) \right|^2 \quad (14)$$

#### 4.3. Application of the EM algorithm

The evaluation of (14) involves a great overhead, not only because the parameters for  $(L_+(l) - L_-(l))$  non-desired combustions must be computed, but for the fact that a non-linear multidimensional search for the  $\delta$ 's in (6) must be carried out.

The EM algorithm offers an alternative solution. Using a prior parameter set  $\hat{\underline{\vartheta}}^{[i]}$ , EM first estimates each sound component and then searches for the optimum pressure parameters individually, iterating both steps until convergence. The original multidimensional problem is thus decomposed in a set of simpler ones that are solved in parallel.

In the following, the results from [5] extended to unknown noise variance and particularized to the case in hand are presented.

#### Estimation-Step

For  $\lambda = L_-, \dots, L_+$ , and  $n$  in the current data window (13), approximate the sound components

$$\hat{w}_n = \tilde{y}_n - \sum_{m=L_-}^{L_+} \tilde{y}_{m,n}(\hat{\underline{\vartheta}}_m^{[i]}) \quad (15)$$

$$\tilde{s}_{\lambda,n} = \tilde{y}_{\lambda,n}(\hat{\underline{\vartheta}}_{\lambda}^{[i]}) + \frac{\hat{\sigma}_{\lambda}^{2[i]}}{\hat{\sigma}^{2[i]}} \hat{w}_n \quad (16)$$

#### Maximization-Step

For  $\lambda = L_-, \dots, L_+$ , determine new parameter estimates

$$\hat{\underline{\vartheta}}_{\lambda}^{[i+1]} = \arg \min_{\underline{\vartheta}_{\lambda}} \sum_n \left| \tilde{s}_{\lambda,n} - \tilde{y}_{\lambda,n}(\underline{\vartheta}_{\lambda}) \right|^2 \quad (17)$$

$$\hat{\underline{\vartheta}}^{[i+1]} = (\hat{\underline{\vartheta}}_{L_-}^{[i+1]}, \dots, \hat{\underline{\vartheta}}_{L_+}^{[i+1]})' \quad (18)$$

and calculate the new noise variances

$$\hat{\sigma}_{\lambda}^{2[i+1]} = \frac{1}{N} \sum_n \left| \tilde{s}_{\lambda,n} - \tilde{y}_{\lambda,n}(\hat{\underline{\vartheta}}_{\lambda}^{[i+1]}) \right|^2 + \dots + \hat{\sigma}_{\lambda}^{2[i]} \left( 1 - \frac{\hat{\sigma}_{\lambda}^{2[i]}}{\hat{\sigma}^{2[i]}} \right) \quad (19)$$

$$\hat{\sigma}^{2[i+1]} = \sum_{m=L_-}^{L_+} \hat{\sigma}_{\lambda}^{2[i+1]} \quad (20)$$

Finally, just the current implementation of the M-step (17) remains to be sketched.

Three amplitudes and a non-linear parameter  $\delta$  must be determined for each  $\lambda$ . Simplifying the notation again and considering that the actual data window contains  $N$  samples, let us define the vectors  $\tilde{\underline{s}}_{\lambda} = (\tilde{s}_{\lambda,1}, \dots, \tilde{s}_{\lambda,N})'$  and  $\underline{x}_{\lambda} = (x_{\lambda,1}, \dots, x_{\lambda,N})'$ . Similarly, let matrix  $\mathbf{C}$  contain the samples pertaining to the two pressure curves with constant shape,  $\mathbf{C} = [\underline{u}_1, \underline{u}_2]$ , and vector  $\underline{v}(\delta_{\lambda})$  describe the movable lobe centered at  $\delta_{\lambda}$ . Filtering the pressure components with the transfer function  $H_{\lambda}(\cdot)$  yields  $\tilde{\mathbf{C}}$  and  $\tilde{\underline{v}}(\delta_{\lambda})$ , respectively. Then, using common algebra operations and the properties of projection matrices, it is easy to show that

$$\hat{\delta}_{\lambda} = \arg \max_{\delta_{\lambda}} \frac{(\tilde{\underline{v}}(\delta_{\lambda})' \mathbf{P}_{\tilde{\mathbf{C}}}^{\perp} \tilde{\underline{s}}_{\lambda})^2}{(\tilde{\underline{v}}(\delta_{\lambda})' \mathbf{P}_{\tilde{\mathbf{C}}}^{\perp} \tilde{\underline{v}}(\delta_{\lambda})) (\tilde{\underline{s}}_{\lambda}' \mathbf{P}_{\tilde{\mathbf{C}}}^{\perp} \tilde{\underline{s}}_{\lambda})}, \quad (21)$$

where  $\mathbf{P}_{\tilde{\mathbf{C}}}^{\perp}$  is the projection matrix onto the space orthogonal to the one spanned by the columns of  $\tilde{\mathbf{C}}$ . The term  $(\tilde{\underline{s}}_{\lambda}' \mathbf{P}_{\tilde{\mathbf{C}}}^{\perp} \tilde{\underline{s}}_{\lambda})$ , constant in  $\delta_{\lambda}$ , was introduced to show the similarity of (21) with a correlation factor. Once  $\hat{\delta}_{\lambda}$  is known, the linear parameters are calculated

$$\hat{\mathbf{D}}' \tilde{\mathbf{D}} \cdot (\alpha_1, \alpha_2, \alpha_3)' = \tilde{\mathbf{D}}' \tilde{\underline{s}}_{\lambda}, \quad (22)$$

with  $\tilde{\mathbf{D}} = [\tilde{\mathbf{C}}, \tilde{\underline{v}}(\hat{\delta}_{\lambda})]$ .

One last remark concerning EM should be made before proceeding to the last section. Notice how the algorithm not only simplifies the computation of the parameter estimates, it also exploits the data more efficiently. Since consecutive data windows overlap, prior estimates of the pressure traces can be used in a twofold manner: first, as good initial estimates for the combustions contained in the current window; second, to “clean” the sound signal, since the  $l$ -th window contains less information about past combustions and therefore they would be estimated less accurately. Both strategies save computations and speed up the convergence.

## 5. EXPERIMENTAL RESULTS

The measurement data were collected from a four cylinder, 1.8 l, turbo charged, spark ignition test bed engine. All cylinders were equipped with a spark plug with integrated pressure sensor. Four acceleration sensors were mounted on the intake side of the engine approximately 10 mm below the cylinder head, each one close to the axis of one of the cylinders. Additionally, the crank angle was measured via a crankshaft sensor. After appropriate filtering, all the signals were downsampled to 2.5 kHz.

Due to the lack of space, the performance of the proposed method can only be illustrated exemplarily by processing the sound

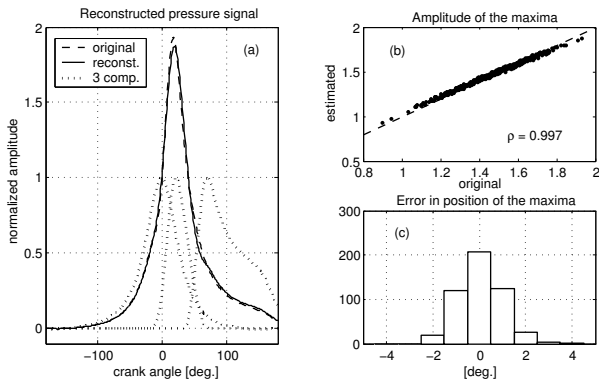


Fig. 2. Parametric pressure model, results with training data.

signal from the sensor at cylinder one, for high load and for the relatively high engine speed of 4,000 rpm. A training data set with 30,000 samples was processed to identify the transfer functions (3), for which impulse response lengths of  $M_A = 25$  and  $M_H = 45$  were selected. 100 misfired and 500 normal combustions were first interpolated and then heuristically combined to produce the three curves pertaining to the parametric pressure model (6). Figure 2 shows the results after reconstructing the 500 combustions used for training. In Fig. 2(a), the worst reconstructed pressure trace is plotted together with the normalized shape of the three components. On the right hand side, a scatter plot asserts the good correlation between original and estimated amplitude of the maxima (b). Below, a histogram displays the error committed when estimating the position of the pressure maxima (c), having an average value of  $0.07^\circ$  and a standard deviation of  $0.98^\circ$ . The model is then able to describe the pressure traces satisfactorily with a minimal set of parameters.

A different data set at the same operating conditions was used to test the reconstruction algorithm. The search for  $\delta$  in (21) was performed using a grid with  $1^\circ$  separation. EM was iterated until the  $\delta$  estimates from all but the two last combustions in the  $l$ -th data window (those with indices  $L_+(l)$  and  $L_+(l) - 1$ ) remained unchanged. After convergence, the current estimate for the  $l$ -th pressure trace was removed from the system and used to clean the sound signal. Besides, to further speed up the system, the linear parameters were jointly estimated by solving (14) instead of using (22).

Figure 3 summarizes the results obtained after evaluating 1000 combustions. Two signals were considered: the first one consisted of the synthetic superimposition of the pressure traces from the 4 cylinders, aiming to determine the hypothetical capability of the system when dealing with “pure” pressure signals; the second one was the sound signal from sensor 1, as already mentioned.

The scatter plots in the upper half of the figure confirm that the parametric model performs well when working with the aggregate pressure (a). The dispersion of the estimated pressure maxima shows that the processing of the sound signal is significantly more challenging (b). Nevertheless, the misfired combustions still cluster together in the low left corner of the picture, making the reconstructed pressure a possible candidate for a misfire detection scheme.

The lower half of figure 3 shows the histograms of the error committed when estimating the position of the pressure maxima. The negligible degradation of (d) compared to (c) asserts the po-

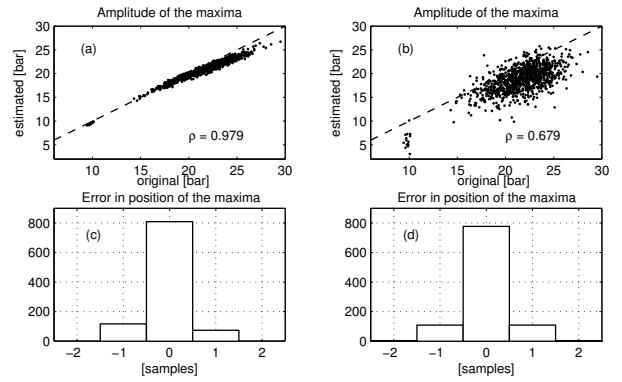


Fig. 3. Reconstruction results using superimposed pressure, left, and sound, right, as input signals.

tential of the reconstructed pressure to serve in closed loop schemes for spark ignition timing [1]. Without forgetting that under the current conditions a sampling period corresponds on average to  $9.6^\circ$  crank angle, the reconstruction yields an error with mean  $0.04^\circ$  and a standard deviation of  $4.78^\circ$ .

## 6. CONCLUSIONS

The EM algorithm perfectly matches the needs of the addressed problem. Together with the parametric pressure model, the procedure yields fast and reliable estimates that make a future real-time implementation conceivable. Better results are expected by combining several sound sensors to jointly reconstruct the pressure and reduce the variance of the amplitude estimates. The EM framework facilitates its implementation, since just a scenario with a single combustion must be evaluated. More details, including a statistical test to perform misfire detection, will be given in a future paper.

## 7. REFERENCES

- [1] J.D. Powell, “Engine control using cylinder pressure: Past, present and future,” *Journal of Dynamic Systems, Measurement and Control*, vol. 115, pp. 343–359, June 1993.
- [2] L. Eriksson, L. Nielsen, and M. Glavenius, “Closed loop ignition control by ionization current interpretation,” *SAE SP-1236*, pp. 159–166, 1997, (SAE Technical Paper 970854).
- [3] German patent application no. DE 198 45 232.2 and PCT/DE 99/02348 (US,JP,EP), “Verfahren und Anordnung zur Bewertung von Verbrennungsvorgängen an einer Brennkraftmaschine,” Applicant: Robert Bosch GmbH, Stuttgart, Germany. Inventors: M. Wagner, J.F. Böhme, J. Förster and R. Raichle, September 1998.
- [4] M. Wagner, J.F. Böhme, and J. Förster, “In-cylinder pressure estimation from structure-borne sound,” *Electronic Engine Controls 2000: Controls (SP-1500)*, pp. 227–235, March 2000, (SAE Technical Paper 2000-01-0930).
- [5] M. Feder and E. Weinstein, “Parameter estimation of superimposed signals using the EM algorithm,” *IEEE Trans. Acoust., Speech, Sig. Proc.*, vol. 36, no. 4, pp. 477–489, April 1988.
- [6] T. Söderström and P. Stoica, *System Identification*, Prentice Hall International, Hemel Hempstead, UK, 1989.